

Bromination of Chalcone: A Study on Synthesis, Characterization, and Optoelectronic Properties

Kosrat N. Kaka¹, Rebaz A. Omer¹, Dyari M. Mamand² and Aryan F. Qader^{1*}

¹Department of Chemistry, Faculty of Science and Health, Koya University, Danielle Mitterrand Boulevard, Koya KOY45, Kurdistan Region – F.R. Iraq

²Department of Physics, College of Science, University of Raparin, Sulaymani, Kurdistan Region – F.R. Iraq

Abstract—In this research work, a new compound, namely 2,6-dibromo-2,6-bis(bromo(phenyl)methyl)cyclohexanone (1), is synthesized and characterized for possible applications in organic electronic devices. The formation of the compound was confirmed by Fourier-transform infrared spectroscopy, ¹H-, and ¹³C-NMR spectroscopy measurements. Furthermore, the spectroscopic and optoelectronic properties of the chemical compound were theoretically investigated using density-functional theory (DFT). Herein, the B3LYP/cc-pVDZ level was used to discover the compound electrostatic potentials and frontier molecular orbitals. The theoretical investigations predicted by DFT were compared with the experimentally obtained results from the ultraviolet visible spectra of the compound after being dissolved in various solvents. Results showed that the experimental band-gap energy of the compound is 3.17 eV, whereas its theoretical value was calculated to be 3.33 eV. The outcome of the achieved results suggests the viability of 2,6-dibromo-2,6-bis(bromo(phenyl)methyl)cyclohexanone for possible applications in organic electronic devices.

Index Terms—Bromination of Chalcone, Density-functional theory, Optoelectronic, Molecular reactivity, Ultraviolet visible.

I. Introduction

Chalcones exhibit a wide range of diverse biological activities. These substances can be easily manufactured or found naturally, but there has been no recent review describing the therapeutic (and on occasion, dystherapeutic) activities of this Chalcone (Elias, et al., 1999; Rani, et al., 2019). Chalcone is a naturally occurring substance that exhibits many pharmacological properties, including anticancer activity. One intriguing mechanism is its ability to alter the production of return on sales (ROS). Pyroptosis has long had anti-cancer

properties. Adding a unit of a,β-unsaturated ketone to chalcone may be a successful method for creating chemotherapeutic medicines (Zhu, et al., 2018; Tajuddeen, et al., 2018). Using various substituted amines in basic conditions, a variety of β-chalcone derivatives was produced through the Claisen-Schmidt condensation procedure. Density-functional theory (DFT) has been optimized for HOMO-LUMO energy calculations using β-chalcones. Vertical excitation energies, absorption wavelengths, and oscillator strengths of the β-chalcone derivative were determined using an optimal time-dependent DFT analysis (Arif, et al., 2020; Priya, et al., 2019). Another class of Chalcone derivatives CO-CH=CH- is regarded as a desirable species since it has a ketoethylenic component moiety. Chalcones and their derivatives have a wide range of antiproliferative, antifungal, antibacterial, antiviral, antileishmanial, antimalarial pharmacological activities, antitubercular, antioxidant, and anti-inflammatory because they contain a reactive unsaturated carbonyl group (Elkanzi, et al., 2022; Tekale, et al., 2020). The chalcones undergo several reactions since they contain C=C and C=O active sites, for example, dibromo compounds formation by the reactions with bromine (Lévai, 2004; Haji, 2013). An environmentally friendly method for brominating chalcones was developed by combining a number of acetophenone derivatives with aromatic aldehydes. Tetrabutylammonium tribromide helped to simplify this process. The antibacterial activity of each produced chalcone dibromide was tested against *Aspergillus flavus*, *Rhizopus* sp., *Fusarium solani*, and *Aspergillus niger*, and Asymmetric bromination of chalcone and benzylideneacetone (trans isomer) in a crystalline β-cyclodextrin complex was studied (Adokar, 2013; Pitchumani, et al., 1994).

Among the modeling methodologies, the DFT formalism stands out because it allows for the calculation of the physicochemical properties of the investigated molecules at a microscopic level with high precision and low processing cosine (Parlak, et al., 2022). This quantum approach, for example, can determine the molecule's frontier orbitals, nucleophilic and/or electrophilic sites, kinetics, and thermodynamic properties (Koparir, et al., 2022b; Rebaz, et al., 2021). The DFT method can compute the geometric optimization of organic molecules. Infrared (IR) spectra and

ARO-The Scientific Journal of Koya University
Vol. XII, No. 1 (2024), Article ID: ARO.11431. 6 pages
DOI: 10.14500/aro.11431

Received: 07 October 2023; Accepted: 02 January 2024
Regular research paper: Published: 28 February 2024

Corresponding author's email: aryan.qader@koyauniversity.org
Copyright © 2024 Kosrat N. Kaka, Rebaz A. Omer, Dyari M. Mamand and Aryan F. Qader. This is an open access article distributed under the Creative Commons Attribution License.



frontier molecular orbitals simulated can be generated for electronic characterization and the generation of quantum reactivity descriptors to comprehend the overall reaction of the molecule's behavior as a nucleophile or electrophile (Omer, et al., 2022b; Omer, et al., 2022c).

The principal aim of this investigation is to comprehensively assess the efficacy of the organic compounds under examination, with a particular focus on their optoelectronic characteristics. The research aims to elucidate the interaction mechanisms between these organic compounds and light, a parameter of paramount importance in various applications such as sensors, solar cells, and light-emitting devices. To deepen our comprehension of the structural attributes of these organic compounds, the B3LYP/cc-pVDZ method is employed in this study. The evaluation entails the examination of the ultraviolet (UV) spectrum of the organic compounds in four distinct solvents. Furthermore, the exploration of the energy band of the target molecule in an alternative solvent serves a dual purpose.

II. EXPERIMENTAL

A. Physical Measurements

The $^1\text{H-NMR}$ spectrum in DMSO- d_6 was recorded with a Bruker F2-processing parameter (SF-300 MHz) spectrometer. The melting point was determined using the BUCHI B-540 apparatus.

B. Synthesis of Title Compound (1)

Preparation of compound (1). Preparation involves mixing 1 mole of 2,6-dibenzylidenecyclohexanone (Chalcone) in 10 ml of chloroform as a solvent with (0.1 ml) of (bromine, 96%) in 10 ml of the same solvent (Chloroform), then stirring for 1 h at room temperature. Finally, the solvent was evaporated using a rotary evaporator, and the precipitate was dried and recrystallized in acetone (if the precipitate became gelatin, use petroleum ether and a refrigerator to cool until 1 day to liquidate the gelatin precipitate) (Fig. 1). The structure of the product compound (1) was identified using Fourier-transform infrared spectroscopy (FT-IR), $^1\text{H-NMR}$, and $^{13}\text{C-NMR}$ instruments. Color is red-yellow; yield is 60%; melting point 105–106°C; FT-IR (KBr, cm^{-1} , ν): 1449 (C=C), 1717 ($\nu\text{C=O}$), 625 ($\nu\text{C=Br}$), 984 ($\nu\text{C-C}$); $^1\text{H-NMR}$ (300 MHz, DMSO- d_6 , δ , ppm): 2.261 (m, 2H, CH_2 -Cyclo-none), 1.816 (m, 2H, CH_2 -Cyclo-none), 6.095 (s, 2H, CH-Br), 7.319 (dd, 10H, Ar-H); $^{13}\text{C-NMR}$ (100 MHz, DMSO- d_6 , δ , ppm): 16.839, 34.59, 55.86, 66.45, 198.17, 136.47.

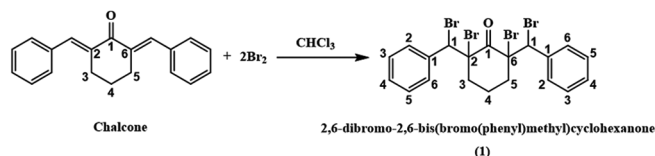


Fig. 1. Reaction pathway for the synthesis of compound (1).

C. Computational Details

Gaussian 09 used a theoretical investigation to calculate quantum computing theory (Medvedev, et al., 2017; Omar, et al., 2023). DFT rounded calculations with the first basis set, cc-pVDZ. Becky's three functional hybrid exchange restrictions (B3LYP) are functional (Becke, 1996; Parlak, et al., 2022). After optimizing the structure of compound (1), a quantum computational calculation can get an excitation state. UV-visible (UV-Vis) is more suitable for investigating optoelectronic behaviors that can benefit from maximum UV-Vis absorption. In the high absorption graph region, the highest peak has the most effective, predictable excitation state. It is possible to predict or show an excitable state in the amount of oscillator strength that is related to the highest peak intensity, as shown in some different solvents.

III. RESULTS AND DISCUSSION

A. NMR Characterization

Compound (1) was synthesized by the reaction of two moles of bromine with Chalcone in chloroform as a solvent. The formation of the products was confirmed based on their FT-IR, $^1\text{H-}$, and $^{13}\text{C-NMR}$ spectroscopy. The IR spectrum for compound (1) showed a strong band at 1717 cm^{-1} , which corresponded to the C=O stretching vibration, the C=C stretching vibration appeared near 1449 cm^{-1} , and the C-Br stretching vibration appeared near 625 cm^{-1} . The $^1\text{H-NMR}$ showed multiple signals at $\delta 2.225$ ppm for the four protons of the cyclohexanone (H2, H4), whereas (H3) showed the pentest signal because of the two protons at $\delta 1.837$ ppm, (H8, H9) showed a singlet signal for the two protons at $\delta 6.240$ ppm, and the (Ar-H) showed multiple signals for the five aromatic protons between 7.703 and 7.951 ppm. The $^{13}\text{C-NMR}$ spectrum showed a variable peak, which is attributed to the following carbons: (C3) at $\delta 16.839$ ppm, (C2, C4) at $\delta 34.592$ ppm, (C8, C9) at $\delta 55.861$ ppm, (C1, C5) at $\delta 66.453$ ppm, (C6) at $\delta 198.178$ ppm, and (Ar-C) at $\delta 136.472$ ppm.

B. UV-Vis Spectroscopy Characteristics of Compound (1) Dissolved in Different Solvents

UV-Vis has a wide range of applications today. It is a scientific category that includes arrangements. It entails studying the electromagnetic radiation of materials besides light. The significance of UV-Vis application stems from its ease and usefulness in investigating the optical and structural properties of materials, such as polymers and polymer nanostructures, as well as light-emitting organic materials. The UV spectrum can depict the material sample's basic electronic behavior. The theoretical calculation associated with the DFT approximation corresponds to the absorption spectra and optical density of the compound (1) molecule, dissolved in different solvents. Each theoretical and experimental approach has more similarities that are close to the amount of the result value. As shown in Fig. 2, the experimental result of UV toward the highest peak is 320.93 nm in dimethyl sulfoxide and the second is 319.97 nm

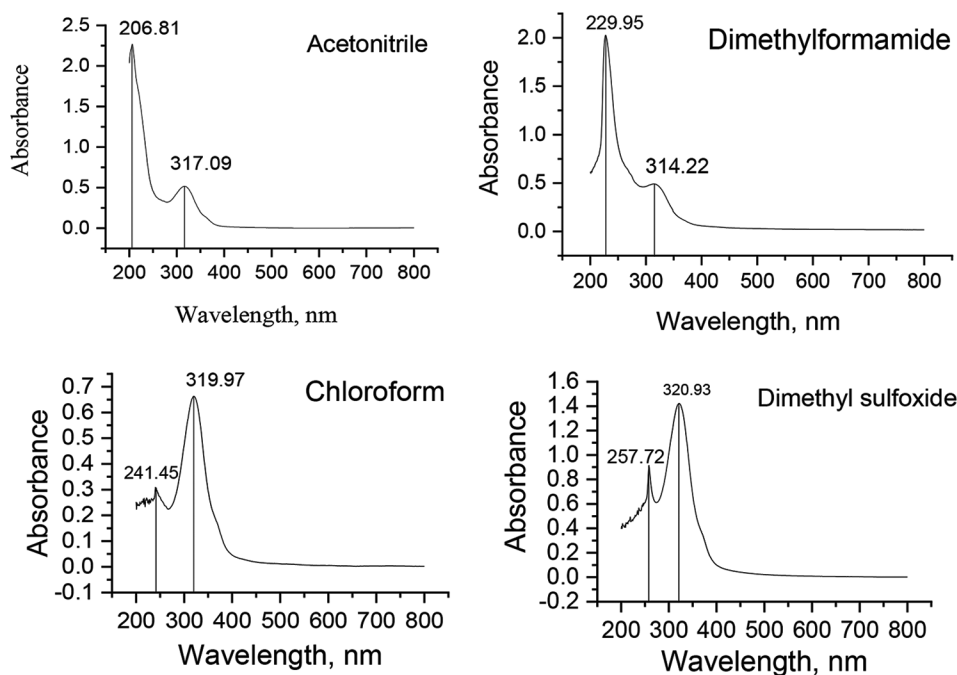


Fig. 2. Experimental ultra-violet visible of compound (1) using different solvent.

in chloroform. However, when compared to the theoretical result, good similarities are shown. The highest peak was observed in chloroform, which is equal to 331.25 nm, and the second highest peak was observed at 330 nm in dimethyl sulfoxide. The experimental ultraviolet result (in DMSO as an example) revealed only two peaks in two different ranges: The first at 320.93 nm and the second peak at 257.72 nm, which are very close to the visible region of light.

As shown in theory (Fig. 3), the first peak in acetonitrile solvent was determined at 329.61 nm with an oscillator strength of 0.0005, whereas the peak in dimethyl formamide was observed at 330.43 nm with an oscillator strength of 0.0005. For both chloroform and dimethyl sulfoxide solvents, the peaks were determined at 331.25 and 330.43 nm with an oscillator strength of 0.0005 and 0.0005, respectively. When the wavelength value approaches 800 nm, the absorbance of compound (1) in the ultraviolet range is experimentally nearly constant. Here, DMSO is a significantly excellent solvent rather than other solvents.

Extremely important for semiconductors is the ability to express the basic property of light absorption of materials in the absorption's expression, where α is absorbance, E_g is band gap, and $h\nu$ is photon energy (Kumara, et al., 2013; Salih, et al., 2023). The optical transition of a semiconductor associated with a forbidden bandwidth or optical band gap can be detected and expressed using the equation below.

$$\alpha h\nu = (h\nu - E_g)^m \quad (1)$$

The direct transition is provided by m equal to 1/2, and the prohibited direct transition is provided by m 3/2. The value of m was determined by dividing it in half.

$$\alpha h\nu = (h\nu - E_g)^{\frac{1}{2}} \quad (2)$$

The graph between $(h\nu)^2$ and photon energy (E) was plotted to determine the allowable band gap value, as shown in Fig. 4. The DMSO solvent was chosen to determine the band gap for both experimental and theoretical data. The experimentally band-gap energy value is equal to 3.166 eV. The results show that the title compound is an excellent semiconductor when dissolved in DMSO. Compared to the theoretical method, the experimental band-gap value for DFT/cc-pVDZ is equal to 3.326, as shown in Fig. 4. The theoretical result is very close to the experimental result, and DFT was an acceptable method for measuring band gap with a cc-pVDZ basis set. The results obtained in our practice suggest that the band-gap energy of the title compound is low, making it a good conductor when using chemically doped with p-type and n-type materials. Another factor that influences the ratio band-gap is the type of solvent used. A material's optical transfer properties can be described as permeable, which is a function of it. It follows Lambert-Beer law because the transmitted radiation density is represented by work, which has an inverse relationship with the original material's penetration depth or length, and permeability is determined by the molecule's geometry.

C. Descriptors of Global Reactivity and Frontier Molecular Orbitals

The theory of frontier molecular orbitals uses fine molecular properties through HOMO-LUMO interactions. In the literature, softness, hardness, and electronegativity are used as global reactivity descriptors (Parlak, et al., 2022; Aktaş, et al., 2022; Koparir, Omar, and Koparir, 2022a; Koparir, et al., 2022c; Rebaz, et al., 2022). Fig. 5 shows that the HOMO electrons are delocalized on the dibromocyclohexane and benzene rings, whereas the LUMO

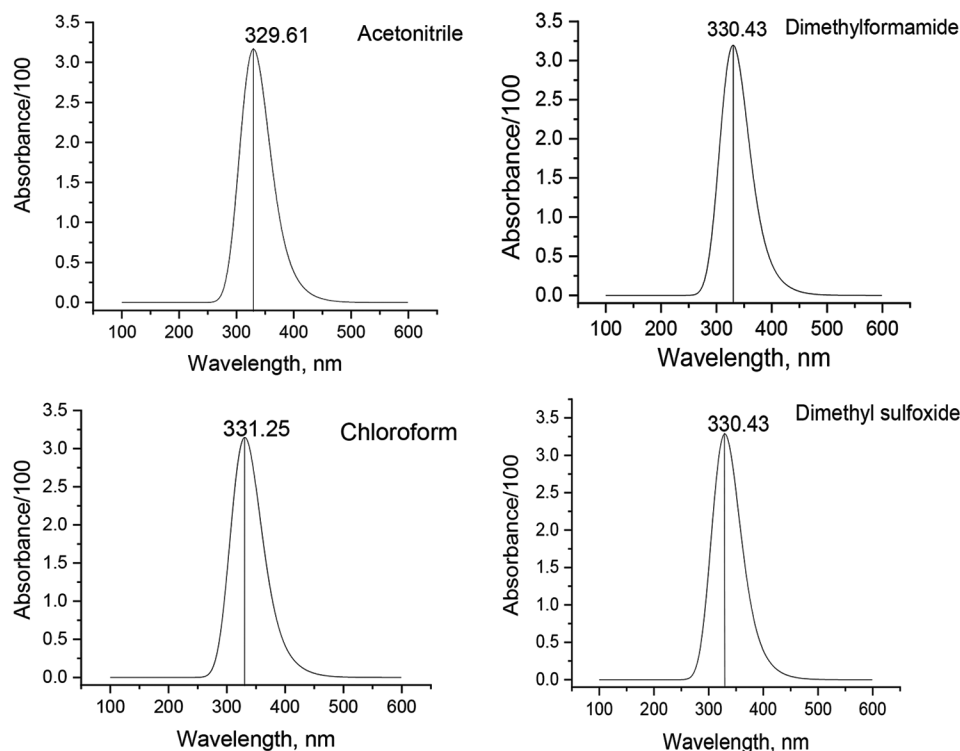


Fig. 3. Theoretical ultraviolet visible of compound (1) using density-functional theory/cc-pVDZ methods.

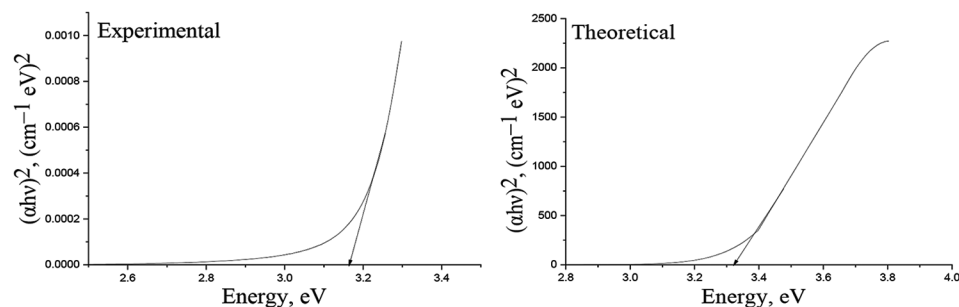


Fig. 4. Band-gap energy $(hv)^2$ plot versus E of compound (1) experimentally and theoretically.

electrons are only delocalized on the cyclohexene ring. The energy separation between the HOMO and the LUMO is 4.325 eV, which shows that the energy gap reflects the molecule's chemical activity. The following parameters for a molecule can be calculated using HOMO and LUMO energy values:

The ionization potential is the amount of energy required to remove an electron from a gaseous atom or molecule. The amount of energy released when an electron is added to a gaseous molecule is defined as electron affinity. Electronegativity is an atom's proclivity to attract electrons. Chemical hardness is a measure of how well molecules resist weight transfer. The molecules with higher chemical hardness values have little or no weight transfer. Table I displays the electronic structure parameter values calculated by the *B3LYP* method with cc-pVDZ.

Because neighboring orbitals in the boundary region may have quasi-degenerate energy levels, only the HOMO and LUMO may not yield a realistic description of the frontier

TABLE I
Descript ors of Global Reactivity for Compound (1)

Parameters	Results (eV) with <i>B3LYP</i> /cc-pVDZ
E_{HOMO}	-6.6861
E_{LUMO}	-2.3611
E_g	-4.325
$I = -E_{HOMO}$ (Plakhutin and Davidson, 2009)	6.6861
$A = -E_{LUMO}$ (Plakhutin and Davidson, 2009)	2.3611
$\chi = (I+A)/2$ (Masoud, et al., 2012)	4.5236
$\eta = (I - A)/2$ (Gökce and Bahceli, 2011)	2.1625
$\sigma = 1/\eta$ (Arivazhagan and Subhasini, 2012)	0.4624
$\Delta E = (E_{LUMO} - E_{HOMO})$ (Jesudason, et al., 2009)	4.325

orbitals. The Gauss Sum 3.0 program does not calculate the density of the mode but displays it from the calculation results of the Gaussian 09 program (Zandiyeh and Ghiasi, 2019). The density of states (DOS) diagram for the title compound is shown in Fig. 6.

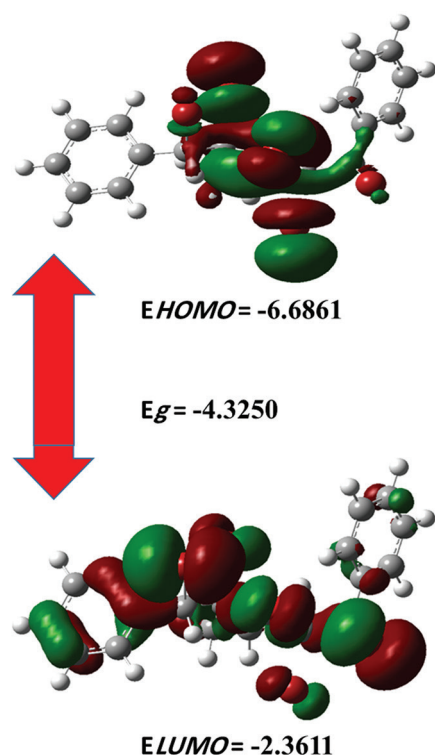


Fig. 5. Energy levels of HOMO and LUMO of the title compound computed at *B3LYP/cc-pVDZ* level in a gas phase.

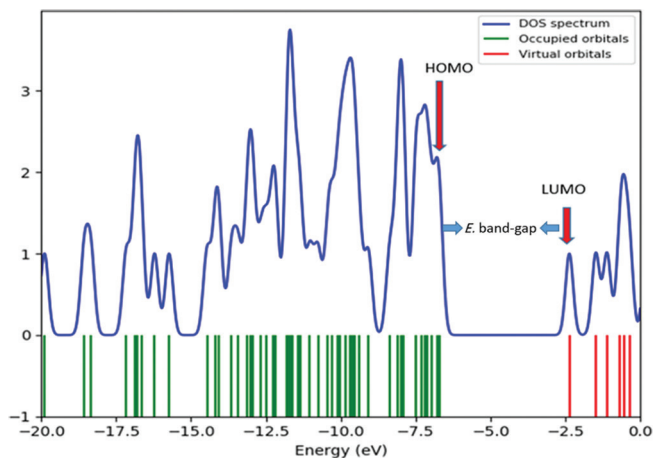


Fig. 6. Density states diagrams for compound (1).

D. Molecular Electrostatic Potential (MEP)

The MEP is linked to the dipole moment, electronegativity, partial charges, and chemical reactivity region of the molecule (Koparir, et al., 2020; Omer, et al., 2022a). It provides a visual method for understanding the molecule's relative polarity. The negative electrostatic potential is the region of the molecule where the electron density is greater than the nucleus (colored in red tones on the ESP surface); the positive electrostatic potential is the region where the electron density is low (the ESP surface is colored in blue tones) (Omer, et al., 2021; Rebaz, et al., 2021; Politzer and Murray, 2002; Rasul, et al., 2023). Fig. 7 shows the MEP map for the title compound. According to the figure, the

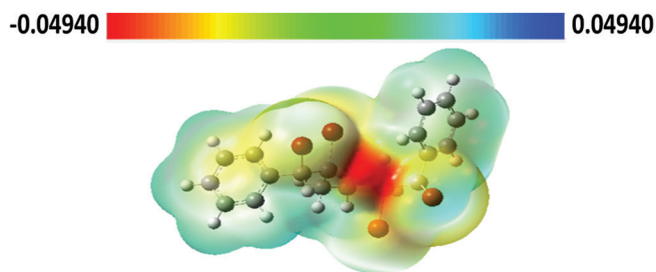


Fig. 7. Molecular electrostatic potential map calculated at *B3LYP/cc-pVDZ* level for compound (1).

negative regions in the molecule are on the two bromine (0.0324 and 0.0247 a.u.), carbon for cyclohexane (0.308, 0.339, 0.006, 0.020, 0.047, and 0.024 a.u.), and oxygen O (0.202 a.u.) atoms. These are the most suitable regions for electrophilic attack. The two benzene rings attached to the cyclohexane ring were the most susceptible to nucleophilic attack in the positive regions.

IV. Conclusion

The compound (1) was synthesized and experimentally reported using FT-IR, ^1H -, and ^{13}C -NMR spectroscopic techniques. The optical and electronic properties of the mentioned compound when dissolved in different solvents are investigated for both experimental and theoretical purposes. The experimental correlation was compared to the theoretical result using the Gaussian 09 program. The compound (1) has an energy gap of 3.166 eV experimentally, but the theoretical result is equal to 3.326 eV. DFT showed good agreement with the experiment results. According to graphs and results estimated from the band-gap value, they have significant similarities. The MEP map shows positive potential locations around carbon atoms of cyclohexane and negative potential locations around bromine atoms.

V. Appendix

Appendixes, if needed, appear before the acknowledgment.

VI. Acknowledgment

Koya University Chemistry Department wishes to express its appreciation to the authors who contributed to their work.

References

- Adokar, M.R., 2013. Synthesis and green bromination of some chalcones and their antimicrobial screening. *International Research Journal of Pharmacy*, 4, pp.194-196.
- Aktaş, A.E., Omer, R.A., Koparir, P., and Koparir, M., 2022. Synthesis, characterization and theoretical anti-corrosion study for substitute thiazole contained cyclobutane ring. *Journal of Physical Chemistry and Functional Materials*, 5, pp.111-120.
- Arif, R., Rana, M., Yasmeen, S., Khan, M.S., Abid, M., and Khan, M.S., (2020). Facile synthesis of chalcone derivatives as antibacterial agents: Synthesis, DNA

- binding, molecular docking, DFT and antioxidant studies. *Journal of Molecular Structure*, 1208, p.127905.
- Arivazhagan, M., and Subhasini, V., 2012. Quantum chemical studies on structure of 2-amino-5-nitropyrimidine. *Spectrochimica Acta Part A: Molecular and Biomolecular Spectroscopy*, 91, pp.402-410.
- Becke, A.D., 1996. Density-functional thermochemistry. IV. A new dynamical correlation functional and implications for exact-exchange mixing. *The Journal of Chemical Physics*, 104, pp.1040-1046.
- Elias, D.W., Beazely, M.A., and Kandepu, N.M., 1999. Bioactivities of chalcones. *Current Medicinal Chemistry*, 6, p.1125.
- Elkanzi, N.A., Hrichi, H., Alolayan, R.A., Derafa, W., Zahou, F.M., and Bakr, R.B., 2022. Synthesis of chalcones derivatives and their biological activities: A review. *ACS Omega*, 7, pp.27769-27786.
- Medvedev, M.G., Bushmarinov, I.S., Sun, J., Perdew, J.P., and Lyssenko, K.A., 2017. Density functional theory is straying from the path toward the exact functional. *Science*, 355, pp.49-52.
- Gökce, H., and Bahceli, S., 2011. A study on quantum chemical calculations of 3-, 4-nitrobenzaldehyde oximes. *Spectrochimica Acta Part A: Molecular and Biomolecular Spectroscopy*, 79, pp.1783-1793.
- Haji, K., 2013. *Kinetics and Mechanistic on the Formation of Some Alpha, Beta-Unsaturated Ketones in Aprotic Solvents and their Reaction with Bromine and Hydrazine*. University of Mousel.
- Jesudason, E.P., Sridhar, S., Malar, E.P., Shanmugapandiyar, P., Inayathullah, M., Arul, V., Selvaraj, D., and Jayakumar, R., 2009. Synthesis, pharmacological screening, quantum chemical and *in vitro* permeability studies of N-Mannich bases of benzimidazoles through bovine cornea. *European Journal of Medicinal Chemistry*, 44, pp.2307-2312.
- Koparir, P., Omar, R., and Koparir, M., 2022a. Synthesis and molecular characterization with DFT: Study of 2-chloro-1-(3-methyl-3-mesityl-cyclobutyl)-ethanone. *Indian Journal of Chemistry*, 61, pp.858-865.
- Koparir, P., Omar, R.A., Sarac, K., Ahmed, L.O., Karatepe, A., Taskin-Tok, T., and Safin, D.A., 2022b. Synthesis, characterization and computational analysis of thiophene-2, 5-diylbis ((3-mesityl-3-methylcyclobutyl) methanone). *Polycyclic Aromatic Compounds*, 43, pp.1-19.
- Koparir, P., Rebaz, O., Karatepe, M., and Ahmed, L., 2020. Synthesis, characterization, and theoretical inhibitor study for (1E, 1'E)-2, 2'-thiobis (1-(3-mesityl-3-methylcyclobutyl) ethan-1-one) dioxime. *El-Cezeri Journal of Science and Engineering*, 8, pp.1495-1510.
- Koparir, P., Sarac, K., and Omar, R.A., 2022c. Synthesis, molecular characterization, biological and computational studies of new molecule contain 1, 2, 4-triazole, and coumarin bearing 6, 8-dimethyl. *Biointerface Research in Applied Chemistry*, 12, pp.809-823.
- Kumara, N., Kooh, M.R.R., Lim, A., Petra, M.I., Voo, N.Y., Lim, C.M., and Ekanayake, P., 2013. DFT/TDDFT and experimental studies of natural pigments extracted from black tea waste for DSSC application. *International Journal of Photoenergy*, 2013, p.109843.
- Lévai, A., 2004. Synthesis of exocyclic α , β -unsaturated ketones. *ARKIVOC*, 2004, pp.15-33.
- Masoud, M.S., Ali, A.E., Shaker, M.A., and Elsalala, G.S., 2012. Synthesis, computational, spectroscopic, thermal and antimicrobial activity studies on some metal-urate complexes. *Spectrochimica Acta Part A: Molecular and Biomolecular Spectroscopy*, 90, pp.93-108.
- Omar, S.Y., Mamand, D.M., Omer, R.A., Rashid, R.F., and Salih, M.I., 2023. Investigating the role of metoclopramide and hyoscine-N-butyl bromide in colon motility. *Journal of Pharmacy and Pharmaceutical Sciences*, 11, pp.109-115.
- Omer, R., Koparir, P., Koparir, M., Rashid, R., Ahmed, L., and Hama, J., 2022a. Synthesis, characterization and DFT study of 1-(3-mesityl-3-methylcyclobutyl)-2-((4-phenyl-5-(thiophen-2-yl)-4H-1, 2, 4-triazol-3-yl) thio) ethan-1-one. *Protection of Metals and Physical Chemistry of Surfaces*, 58, pp.1-13.
- Omer, R.A., Koparir, P., Ahmed, L., and Koparir, M., 2021. Computational and spectroscopy study of melatonin. *Indian Journal of Chemistry*, 60, pp.732-741.
- Omer, R.A., Koparir, P., and Ahmed, L.O., 2022b. Characterization and inhibitor activity of two newly synthesized thiazole. *Journal of Bio-and Tribo-Corrosion*, 8, pp.1-12.
- Omer, R.A., Koparir, P., Qader, I.N., and Ahmed, L.O., 2022c. Theoretical determination of corrosion inhibitor activities of naphthalene and tetralin. *Gazi University Journal of Science*, 35, pp.434-444.
- Parlak, A.E., Omar, R.A., Koparir, P., and Salih, M.I., 2022. Experimental, DFT and theoretical corrosion study for 4-(((4-ethyl-5-(thiophen-2-yl)-4H-1, 2, 4-triazole-3-yl) thio) methyl)-7, 8-dimethyl-2H-chromen-2-one. *Arabian Journal of Chemistry*, 15, p.104088.
- Pitchumani, K., Velusamy, P., Sabithamala, S., and Srinivasan, C., 1994. Modification of chemical reactivity upon cyclodextrin encapsulation: Asymmetric bromination of chalcone and benzylideneacetone. *Tetrahedron*, 50, pp.7903-7912.
- Plakhutin, B.N., and Davidson, E.R., 2009. Koopmans' theorem in the restricted open-shell hartree-fock method. 1. A variational approach. *The Journal of Physical Chemistry A*, 113, pp.12386-12395.
- Politzer, P., and Murray, J.S., 2002. The fundamental nature and role of the electrostatic potential in atoms and molecules. *Theoretical Chemistry Accounts*, 108, pp.134-142.
- Priya, M.K., Revathi, B., Renuka, V., Sathya, S., and Asirvatham, P.S., 2019. Molecular structure, spectroscopic (FT-IR, FT-Raman, ¹³C and ¹H NMR) analysis, HOMO-LUMO energies, Mulliken, MEP and thermal properties of new chalcone derivative by DFT calculation. *Materials Today Proceedings*, 8, pp.37-46.
- Rani, A., Anand, A., Kumar, K., and Kumar, V., (2019). Recent developments in biological aspects of chalcones: The Odyssey continues. *Expert Opinion on Drug Discovery*, 14, pp.249-288.
- Rasul, H.H., Mamad, D.M., Azeez, Y.H., Omer, R.A., and Omer, K.A., 2023. Theoretical investigation on corrosion inhibition efficiency of some amino acid compounds. *Computational and Theoretical Chemistry*, 1225, p.114177.
- Rebaz, O., Ahmed, L., Jwameer, H., and Koparir, P., 2021. Structural analysis of epinephrine by combination of density functional theory and hartree-fock methods. *El-Cezeri Journal of Science and Engineering*, 9, pp.760-776.
- Rebaz, O., Ahmed, L., Qader, I., and Koparir, P., 2022. Theoretical analysis of the reactivity of carmustine and lomustine drugs. *Journal of Physical Chemistry and Functional Materials*, 5, pp.84-96.
- Rebaz, O., Koparir, P., Qader, I.N., and Ahmed, L., 2021. Structure reactivity analysis for phenylalanine and tyrosine. *Cumhuriyet Science Journal*, 42, pp.576-585.
- Salih, S.K., Mustafa, R.M., Mamad, D.M., Kaka, K.N., Omer, R.A., and Hamad, W.M., 2023. Synthesis of liquid crystalline benzothiazole based derivatives: Theoretical and experimental study of their optical and electrical properties. *ZANCO Journal of Pure and Applied Sciences*, 35, pp.143-162.
- Tajuddeen, N., Isah, M.B., Suleiman, M.A., Van Heerden, F.R., and Ibrahim, M.A., 2018. The chemotherapeutic potential of chalcones against leishmaniasis: A review. *International Journal of Antimicrobial Agents*, 51, pp.311-318.
- Tekale, S., Mashele, S., Poee, O., Thore, S., Kendrekar, P., and Pawar, R., 2020. Biological role of chalcones in medicinal chemistry. In: *Vector-Borne Diseases-Recent Developments in Epidemiology and Control*. IntechOpen, London.
- Zandiyeh, Z., and Ghiasi, R., 2019. A theoretical approach towards identification of external electric field effect on (η^5 -C₅H₅) Me₂Ta (η^2 -C₆H₄). *Russian Journal of Physical Chemistry A*, 93, pp.482-487.
- Zhu, M., Wang, J., Xie, J., Chen, L., Wei, X., Jiang, X., Bao, M., Qiu, Y., Chen, Q., Li, W., Jiang, C., Zhou, X., Jiang, L., Qiu, P., and Wu, J., 2018. Design, synthesis, and evaluation of chalcone analogues incorporate α , β -Unsaturated ketone functionality as anti-lung cancer agents via evoking ROS to induce pyroptosis. *European Journal of Medicinal Chemistry*, 157, pp.1395-1405.